than likely the observed isotope effect arises from both reaction channels being operative, a notion which is consistent with the results of our previously reported quantitative molecular orbital calculations.[9]

## Conclusions

The following conclusions may be drawn from the study reported in this paper:

1. The direction of the secondary deuterium isotope effects in proton transfer processes involving a variety of simple alkyl benzenes (e.g., toluene, the xylenes, and mesitylene) is consistent with the notion that a methyl group para to the site of reaction acts through hyperconjugation to stabilize the positive charge. The hyperconjugative arguments would lead to assignment of the same direction for the isotope effect of an ortho disposed methyl substituent. However, our measurements indicate for the ortho position the opposite, suggesting the dominance of other factors in determining the overall isotope effect.

2. Contributions to the total isotope effect caused by methyl groups meta to the protonation site appear to be very small. This is in line with the results of simple resonance theory, where in drawing the contribution valence structures

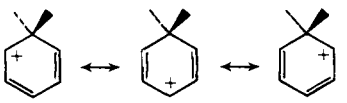

we imply that the molecule's positive charge resides largely on the ortho and para sites.

3. The measured isotope effect on the proton transfer reaction involving *p*-xylene seems to require ipso protonation of at least some (if not all) of the molecules.

## Experimental Section

Toluene-$\alpha$-$d_1$ was prepared by the method of Trevoy and Brown,[16] by reacting benzyl bromide (4 g) in THF (25 ml.) with $LiAlD_4$ (1 g) at room temperature. Toluene-$\alpha$-$d_3$ and *o*- and *m*-xylene-$\alpha$-$d_6$ were prepared by reacting benzene (10 ml) with $AlCl_3$ and $CD_3I$ at 0 °C for 96 h.[17] Separation was effected by gas chromatography.[18] Mesitylene-$\alpha$-$d_9$ was prepared as above except that the reaction mixture was heated to 100 °C for 3 h. The product was purified by gas chromatography. *p*-Xylene-$\alpha$-$d_6$ was purchased from Aldrich.

**Acknowledgments.** The authors express their gratitude to Professors Halevi and Wolfsberg for stimulating discussions during the course of this research. Professors Brandt and Miller are thanked for their help with the separation of the xylenes. This research was supported in part by grants from the National Science Foundation and from the Research Corporation.

## References and Notes

(1) (a) University of California Regents Intern Fellow, 1974–1978; (b) Alfred P. Sloan Fellow, 1974–1976.
(2) (a) E. S. Lewis, R. R. Johnson, and G. M. Coppinger, *J. Am. Chem. Soc.*, **81**, 3140 (1959); (b) V. J. Shiner, Jr., and C. J. Verbanic, *ibid.*, **79**, 373 (1957). For reviews, see: (c) V. J. Shiner, *ACS Monogr.*, **No. 167**, 90 (1970); (d) D. E. Sunko and S. Borcic, *ibid.*, **No. 167**, 160 (1970).
(3) J. W. Timberlake, J. A. Thompson, and R. W. Taft, *J. Am. Chem. Soc.*, **93**, 274 (1971).
(4) For a discussion of the application of the perturbation molecular orbital theory to the structures of carbocations, see: W. J. Hehre, *Acc. Chem. Res.*, **8**, 369 (1975).
(5) W. A. Lathan, W. J. Hehre, and J. A. Pople, *J. Am. Chem. Soc.*, **93**, 808 (1971).
(6) J. F. Wolf, J. L. Devlin, III, R. W. Taft, M. Wolfsberg, and W. J. Hehre, *J. Am. Chem. Soc.*, **98**, 287 (1976).
(7) Trapped ion cyclotron resonance spectroscopy. Method: (a) R. T. McIver, Jr., *Rev. Sci. Instrum.*, **41**, 555 (1970); (b) J. D. Baldeschwieler and S. S. Woodgate, *Acc. Chem. Res.*, **4**, 114 (1971); (c) R. T. McIver, Jr., and R. C. Dunbar, *Int. J. Mass Spectrom. Ion Phys.*, **7**, 471 (1971). Representative applications: (d) M. T. Bowers, D. H. Aue, H. M. Webb, and R. T. McIver, Jr., *J. Am. Chem. Soc.*, **93**, 4314 (1971); (e) R. T. McIver, Jr., and J. R. Eyler, *ibid.*, **93**, 6334 (1971); (f) R. T. McIver, Jr., and J. H. Silvers, *ibid.*, **95**, 8462 (1973); (g) R. T. McIver, Jr., and J. S. Miller, *ibid.*, **96**, 4323 (1974); (h) W. J. Hehre, R. T. McIver, Jr., J. A. Pople, and P. v. R. Schleyer, *ibid.*, **96**, 7162 (1974); (i) J. F. Wolf, P. G. Harch, R. W. Taft, and W. J. Hehre, *ibid.*, **97**, 2902 (1975).
(8) (a) W. J. Hehre and J. A. Pople, *J. Am. Chem. Soc.*, **94**, 6901 (1972); (b) W. C. Ermler, R. S. Mulliken, and E. Clementi, *ibid.*, **98**, 388 (1976).
(9) J. L. Devlin, III, J. F. Wolf, R. W. Taft, and W. J. Hehre, *J. Am. Chem. Soc.*, **98**, 1990 (1976); see also ref 7h.
(10) For a recent review of steric isotope effects, see: R. E. Carter and L. Melander, *Adv. Phys. Org. Chem.*, **10**, (1973).
(11) W. J. Hehre, R. F. Stewart, and J. A. Pople, *J. Chem. Phys.*, **51**, 2657 (1969).
(12) All calculations have been performed using the GAUSSIAN 70 series of computer programs. W. J. Hehre, W. A. Lathan, R. Ditchfield, M. D. Newton, and J. A. Pople, program No. 236, Quantum Chemistry Program Exchange, Indiana University, Bloomington Ind.
(13) Other geometrical parameters are fixed at "standard model" values: for toluene, ref 14; for protonated toluene, ref 7h.
(14) J. A. Pople and M. S. Gordon, *J. Am. Chem. Soc.*, **89**, 4253 (1967).
(15) R. W. Taft, "Proton Transfer Reactions", E. F. Caldin and V. Gold, Ed., Chapman and Hall, London, 1975, p 31.
(16) L. W. Trevoy and W. G. Brown, *J. Am. Chem. Soc.*, 71, 1675 (1959).
(17) J. F. Norris and D. Rubinstein, *J. Am. Chem. Soc.*, **61**, 1163 (1939).
(18) J. V. Mortimer and P. L. Gent, *Anal. Chem.*, **36**, 754 (1964).

# Determination of Precise and Reliable Gas Diffusion Coefficients by Gas Chromatography

**Frank Yang, Stephen Hawkes,* and F. T. Lindstrom**

*Contribution from the Department of Chemistry, Oregon State University, Corvallis, Oregon 97331.* *Received February 16, 1976*

**Abstract:** A specially designed gas chromatograph has been tested for the measurement of the diffusion coefficient of methane in helium at 25 °C. Both the continuous elution and Knox's arrested elution techniques were used and the latter is considered the more reliable, yielding a value of 0.6735 averaged over seven arrested times with a standard deviation of 0.0008. The equation for the elution profile of an arrested elution peak is derived and experimental peaks fit this with a standard error near $7 \times 10^{-4}$. Uncertainty in the pressure measurement decreases the reliability of the result but a value of $0.674 \pm 0.002$ is confidently reported; this agrees well with other published data.

Gaseous binary molecular diffusion coefficients $D_g$ are an important physical parameter in both basic and engineering research and in chromatographic theory. Various theoretical and experimental approaches are employed for their measurement and numerous reports have been published since the early years of this century. However, the results obtained from

different researchers have always deviated to some extent from each other. It is the intention of this investigation to explore the possibility of obtaining highly precise and accurate $D_g$ values by a carefully designed GC system, and by employing a computer for accurate data collection and for least-squares fitting of the theoretical zone dispersion equation.

The experimental approaches employed here were Giddings' continuous elution method[1-3] and its arrested elution modification invented by Knox and McLaren.[4] The consistency of the results obtained from the above two methods serves as a convincing indicator of the accuracy of the $D_g$ values obtained. Also, the efficiency and performance of the GC system can be explored. A brief discussion of both methods is given below.

(A) **Continuous Elution Method.** This was first introduced and demonstrated by Giddings and Seager.[1-3] Recent reviews of this method and its modified approaches are given by Marrero and Mason[5] and Maynard and Grushka.[6] The continuous elution method for the determination of $D_g$ is generally conducted in an open tube with circular cross section. The average carrier stream velocity is chosen such that the plate height depends principally on only one of the terms in the Taylor equation: the longitudinal diffusion term (Van Deemter's $B/v$ term) or the mass transfer term (Van Deemter's $Cv$ term). The advantage of this method is that the speed of collecting data is very rapid and the precision is comparable to or even better than most of the other methods used so far. Giddings and Seager[3] demonstrated that 200 separate determinations can be obtained in 36 h while maintaining a precision of about 1%. The speed can even be faster if a shorter column is employed. However, an inherent weakness of this method is that zone broadening factors such as racetrack, secondary flow, concentration effect, end effect, and the buoyant effect of the solute-solvent pair, etc., cannot be isolated in the same run of the experiment. The correction of these extra zone broadening factors may need specially designed systems or the use of two different length columns in two experiments conducted under the same conditions, as in the end effect correction as introduced by Giddings and Seager.[3] The plate height due to end effects may then be calculated from the equation

$$H_{end} = (L_d - L_c)\left[\frac{\tau_d^2 - \tau_c^2}{(t_d - t_c)^2}\right] \qquad (1)$$

where $L_d$ and $L_c$ are the lengths of the principal and correction columns, and $(\tau_d^2 - \tau_c^2)$ and $(t_d - t_c)$ are the corresponding differences for the second and first moments of the time base. Identity of two separate sets of experimental conditions (velocity, inlet and outlet pressure, temperature, sample concentration, etc.) is very difficult to achieve especially after the exchange of the column. The correction of extra zone broadening factors in the continuous elution method therefore becomes a very difficult task for precision work.

(B) The arrested elution method as used by Knox and McLaren[4] was basically the same as the continuous elution method except the carrier flow was arrested when the solute zone had migrated about half-way along the column. The solute zone was then allowed free molecular diffusion for a time, $t_2$, and finally eluted from the column by resuming the carrier flow. The experiment was repeated for the same velocity and different arrested times. The total variance measured was then plotted against the arrested time. The slope of the resulting straight line is $2D_g/v^2$, and therefore by knowing the average carrier velocity, $v$, the binary molecular diffusion coefficient, $D_g$, can be calculated. The advantage of using the arrested elution method is that the effects of zone broadening other than axial molecular diffusion and nonuniform flow profile do not affect the result, and therefore, the end effect correction as mentioned in the continuous elution method is not necessary. Also, the column can be very short and hence decrease the possible error introduced by the pressure drop between the inlet and outlet of a long column, especially a packed column. Moreover, no assumptions are made about the precise form of the flow profile (which is assumed to be parabolic in the Taylor equation), the smoothness of the column wall, or the accuracy with which the column diameter is known. The disadvantages of this method are that a constant velocity must be maintained over a long period for runs at various arrested times and, with traditional methods of measuring variance in calculating $D_g$, a Gaussian elution peak is assumed. Experimentally, a near Gaussian elution peak may be obtainable but a constant velocity over a period of about 3 h is difficult to obtain. It also has to be recognized that the need for several runs (which may involve a period of 2 to 5 h) to get a $D_g$ value with a precision of about 2% may degrade the purpose of using GC as a rapid method in determining $D_g$ values.

The advantage of the above-mentioned methods may only be appreciated if a single run of the experiment will be sufficient for the measurement of a $D_g$ value with high precision and accuracy. This may be achieved by a direct least-squares fit of the experimental data to the theoretical equation of the eluted concentration profile and computing the best $D_g$ value. This approach may be adapted either to the arrested elution method or the continuous elution method. It also has the additional advantage that any deviations from the expected form of the concentration profile give warning of incorrect design of the experiment or malfunction of the equipment.

The theoretical equations will be given in the following theory.

## Theory

For the arrested elution method, the theoretical expression for solute zone dispersion in a tube of open circular cross section can be obtained by solving the mass balance equation for the following three steps.

**Step One.** In this initial step, a solute sample with an initial concentration $C_0$ and distributed as an assumed plug function is injected into the column. A carrier stream with an average velocity, $v$, carries the solute zone downstream along the column. The distance along the column is considered to be the $z$ coordinate. Consider the zone dispersion is due only to axial (or longitudinal) molecular diffusion, the effect of nonuniform flow profile, and any other continuous processes within the column, and the mass balance equation can be written as

$$\frac{\partial C_1}{\partial t} = D_{eff}\frac{\partial^2 C_1}{\partial z^2} - v\frac{\partial C_1}{\partial z} \qquad \text{for } 0 < z < \infty \qquad (2)$$

where $D_{eff}$ is the overall coefficient of dispersion from all continuous processes within the column, defined as $D_{eff} = \frac{1}{2}(\partial\sigma^2/\partial t)$ where $\sigma^2$ is the variance of the dispersion in units of length$^2$, $C_1$ is the instantaneous concentration at time $t$ and the $z$ is the distance from the injection point.

The initial condition is

$$C(z, 0) = 0 \qquad (3)$$

and the boundary conditions are

$$C(0, t) = C\delta(t) \qquad (4)$$

$$\lim_{z\to\infty} C(z, t) = 0 \qquad (5)$$

Solving eq 2 by Laplace transformation and its inversion theory, we have

$$C_1(z, t) = \left(\frac{C_0 z}{2\sqrt{\pi D_{eff} t^3}}\right)\exp\left(\frac{-(z - vt)^2}{4D_{eff}t}\right) \qquad (6)$$

A general solution for the continuous elution method can be obtained from eq 6 by replacing $z$ by the length of the col-

umn, $L$, between the injection point and the point of detection where $C_1$ is measured. This assumes that the column extends infinitely beyond the point of detection, and it will be seen in the Experimental Section that we have approximated this condition.

**Step Two.** This step will be initiated when the distribution of the above concentration profile is allowed to obtain until the absolute time $t = t_1$ is reached (the center of gravity of the solute zone may be near the center of the column). At this point, we arrest the carrier flow, and reset the time scale to zero again. The mass balance equation at this step may be written as

$$\frac{\partial C_2}{\partial t} = D_g \frac{\partial^2 C_2}{\partial z^2} \qquad \text{for } 0 < z < \infty \tag{7}$$

the initial condition is

$$C_2(z, 0) = C_1(z, t_1) = \frac{C_0 z}{2\sqrt{\pi D_{eff}} t_1^{3/2}} \exp\left(\frac{-(z - vt_1)^2}{4D_{eff}t_1}\right) \tag{8}$$

and the boundary conditions are

$$C_2(0, t) = 0 \tag{9}$$

$$\lim_{z \to \infty} C_2(z, t) = 0 \tag{10}$$

Equation 7 is solved by utilizing the initial and boundary conditions and double Laplace transforms with subsequent inversions. We obtain

$$C_2(z, t) = \frac{C_0 D_{eff} D_g t}{2\sqrt{\pi}\,(D_{eff}t_1 + D_g t)^{3/2}} \times \left\{ \left(\frac{z}{D_g t} + \frac{v}{D_{eff}}\right) \exp\left(\frac{-(z - vt_1)^2}{4(D_{eff}t_1 + D_g t)}\right) - \frac{1}{2}\left(\frac{z}{D_g t} + \frac{v}{D_{eff}}\right) \exp\left(\frac{-(z - vt_1)^2}{4(D_{eff}t_1 + D_g t)}\right) \times \operatorname{erfc}\left(\frac{z\sqrt{D_{eff}t_1/D_g t} + v\sqrt{D_g t t_1/D_{eff}}}{2\sqrt{D_{eff}t_1 + D_g t}}\right) + \frac{1}{2}\left(\frac{z}{D_g t} - \frac{v}{D_{eff}}\right) \exp\left(\frac{-(z + vt_1)^2}{4(D_{eff}t_1 + D_g t)}\right) \times \operatorname{erfc}\left(\frac{z\sqrt{D_{eff}t_1/D_g t} - v\sqrt{D_g t t_1/D_{eff}}}{2\sqrt{D_{eff}t_1 + D_g t}}\right) \right\} \tag{11}$$

Equation 11 gives the solution for the instantaneous concentration profile at a given arrested time $t$. We can set $t = t_2$, equals the total arrested time, and also simplify by neglecting the last two error function terms which are negligible under all conditions we can conceive for this work. Then we obtain a simple solution for the concentration profile after steps one and two

$$C_2(z, t_2) = \frac{C_0 D_{eff}\,(z + vt_2(D_g/D_{eff}))}{2\sqrt{\pi}(D_{eff}t_1 + D_g t_2)^{3/2}} \times \exp\left(\frac{-(z - vt_1)^2}{4(D_{eff}t_1 + D_g t_2)}\right) \tag{12}$$

When the arrested time approaches 0, eq 12 reduces to eq 6. This verifies the correct mathematical derivation.

**Step Three.** This step starts when the total arrested time $t_2$ is reached. The carrier flow resumes at this moment. Again, we reset the time scale to zero and velocity to $v$. The mass balance equation is

$$\frac{\partial C_3}{\partial t} = D_{eff}\frac{\partial^2 C_3}{\partial z^2} - v\frac{\partial C_3}{\partial z} \qquad \text{for } 0 < z < \infty \tag{13}$$

The initial condition is

$$C_3(z, 0) = C_2(z, t_2) \tag{14}$$

and the boundary conditions are

$$C_3(0, t) = 0 \tag{15}$$

$$\lim_{z \to \infty} C_3(z, t) = 0 \tag{16}$$

again using Laplace transformation and the inversion method, we obtain

$$C_3(z, t) = \frac{C_0 D_{eff}}{2\sqrt{\pi}\,(D_{eff}t_1 + D_g t_2 + D_{eff}t)^{3/2}} \times \left\{ \left(z + vt_2\frac{D_g}{D_{eff}}\right) \exp\left(\frac{-(z - v(t_1 + t))^2}{4(D_{eff}t_1 + D_g t_2 + D_{eff}t)}\right) - \frac{1}{2}\left(z + vt_2\frac{D_g}{D_{eff}}\right) \exp\left(\frac{-(z - v(t_1 + t))^2}{4(D_{eff}t_1 + D_g t_2 + D_{eff}t)}\right) \times \operatorname{erfc}\left[\frac{[(z - vt)/2]\sqrt{(D_{eff}t_1 + D_g t_2)/D_{eff}t} + (vt_1/2)\sqrt{D_{eff}t/(D_{eff}t_1 + D_g t_2)}}{\sqrt{D_{eff}t_1 + D_g t_2 + D_{eff}t}}\right] + \frac{1}{2}\left(z - vt_2\frac{D_g}{D_{eff}}\right) \exp\left(\frac{-(z + v(t_1 + t))^2}{4(D_{eff}t_1 + D_g t_2 + D_{eff}t)} + \frac{vz}{D_{eff}}\right) \times \operatorname{erfc}\left[\frac{[(z + vt)/2]\sqrt{(D_{eff}t_1 + D_g t_2)/D_{eff}t} - (vt_1/2)\sqrt{D_{eff}t/(D_{eff}t_1 + D_g t_2)}}{\sqrt{D_{eff}t_1 + D_g t_2 + D_{eff}t}}\right] \right\} \tag{17}$$

Substituting column length, $L$, for $z$, $t_m$ for the time spent mobile $(t_1 + t)$, $C$ for $C_3(z, t)$, neglecting the two error functional terms on the right-hand side of eq 17, we obtain the simplified final form of the solute concentrations profile after the zone was eluted from the column, that is

$$C = \frac{C_0(D_{eff}L + vt_2 D_g)}{2\sqrt{\pi}\,(D_{eff}t_m + D_g t_2)^{3/2}} \exp\left(\frac{-(L - vt_m)^2}{4(D_{eff}t_m + D_g t_2)}\right) \tag{18}$$

A two-parameter least-squares fit of the experimental data to eq 18 would give us $D_g$ and $D_{eff}$ at the same time. However, it was found that $D_{eff}$ and $D_g$ are numerically highly correlated and therefore only a one-parameter least-squares fit would give us a reliable $D_g$ value. Fortunately, the total axial zone dispersity, $D_{eff}$, can be related to the molecular diffusivity at one atmosphere, $D_g^*$, and carrier flow rate, $v$, by using the modified Taylor's equation

$$D_{eff} = \frac{D_g^*}{P_0} + \frac{r^2 v^2 P_0}{48 D_g^*} \tag{19}$$

here $P_0$ is the outlet pressure in atmospheres and $r$ is the radius of the column.

In using this form it is necessary to keep the velocity small so that any errors in the estimate of the mass transfer effect

(the second term in eq 19) can be neglected. It is also important to realize that the pressure correction terms such as the James–Martin factor and Giddings' factor are approaching unity because of the small pressure gradient across the empty column.

Substituting eq 19 into 18, we have

$$C(L,t) = \frac{C_0\left[L\left(\frac{D_g^*}{P_0} + \frac{r^2v^2P_0}{48D_g}\right) + vt_2D_g^*/P_0\right]}{2\sqrt{\pi}\left[\left(\frac{D_g^*}{P_0} + \frac{r^2v^2P_0}{48D_g^*}\right)t_m + t_2D_g^*/P_0\right]^{3/2}} \times \exp\left(\frac{-(L-vt_m)^2}{4\left[\left(D_g^*/P_0 + \frac{r^2v^2P_0}{48D_g^*}\right)t_m + \frac{D_g^*t_2}{P_0}\right]}\right) \quad (20)$$

For a dense packed column or a capillary tube, the pressure correction terms $j$ and $f$ must be entered into eq 19. Also, the pressure gradient in the first and the second elution period must be considered. The final equation will appear more complex in its form but it can be easily derived by a simple mathematical exercise.

The general equation for the continuous elution method can also be obtained from eq 20 by putting $t_2 = 0$, thus

$$C(L,t) = \frac{C_0L}{2\sqrt{\pi\left(\frac{D_g^*}{P_0} + \frac{r^2v^2P_0}{48D_g^*}\right)t^{3/2}}} \times \exp\left(\frac{-(L-vt)^2}{4t\left(\frac{D_g^*}{P_0} + \frac{r^2v^2P_0}{48D_g^*}\right)}\right) \quad (21)$$

By measuring the concentration profile of the dispersed zone at the end of the column, and then fitting these data to the relative theoretical eq 20 or 21, the binary molecular diffusion coefficient at 1 atm, $D_g^*$, can be calculated.

The precision and accuracy of the data obtained from the above theoretical least-squares fit method depend upon the extent of the contribution to the zone broadening due to zone-broadening factors, not included in the equation (such as end effects). Failure in the experimental design is easily detected because it gives rise to systematic deviation of the experimental data from the fitted equation at the tails (and sometimes the maximum) of the peak. Some important causes of error that need to be carefully examined follow.

**(A) Secondary Flow.** For an ideal fluid in laminar flow within a curved column of any cross section, secondary flow may be introduced by the pressure gradient developed across the bend due to the centrifugal force of the fluid moving around the bend. The fluid in the central streamlines is subjected to relatively greater centrifugal force because of its greater axial velocity. The fluid near the center is therefore thrown outward toward the outer wall of the bend. By reason of fluid continuity, it is continuously replaced by the recirculation of fluid along the walls. The net result of this phenomenon is establishment of the spiral motion of secondary flow in a curved column.

In a chromatography column, the effect of secondary flow in contrast to most of the known zone-broadening factors is to enhance the zone dispersion across the cross-sectional plane, and hence minimize the axial zone broadening. A narrower peak would be expected from a strong effect of secondary flow superimposed on the elution peak.

Secondary flow may be indicated by the extra pressure drop, $\Delta p$, across the curved column in comparison to the pressure drop across the straight tube with the same geometry. The larger the pressure drop, the higher the effect of secondary flow. This extra pressure drop, $\Delta p$, may be expressed as

$$\Delta p = (F-1)\frac{8\eta Lv}{r^2} \quad (22)$$

where $\eta$ is the viscosity of the fluid in the column and $F$ is the resistance factor which was given by White[7] as

$$F = 1 \qquad \text{for } K \leq 11.6 \quad (23)$$

and

$$1/F = 1 - [1 - (11.6/K)^{0.45}]^{1/0.45} \qquad \text{for } K > 11.6 \quad (24)$$

where, $K$ is Dean's factor which was given as

$$K = \frac{2\rho vr}{\eta}\left(\frac{2r}{D}\right)^{1/2} \quad (25)$$

$\rho$ is the density of the fluid in the column, and $D$ is the radius of curvature of the coil.

Equation 23 gives the upper limit of $K$ where secondary flow does not occur. Equation 25 is used to estimate the upper limit of flow rate, $v$, that can be used without the introduction of secondary flow, for a given carrier fluid, radius of curvature, radius of the column, and the temperature of the fluid. For example, at 0 °C, for a given coil column with a radius of curvature of 10 cm and a radius of 0.1096 cm the estimated upper flow rate of carrier helium can be as high as 386 cm/s before the effect of secondary flow has to be considered. In general, the effect of secondary flow can be neglected if a sufficiently large radius of curvature of the coil and a low density fluid are employed.

**(B) Giddings' Racetrack Effect.** For high precision work, Giddings' racetrack effect has also to be evaluated if a coiled column is employed. This effect accounts for the coil effect on the linear flow rate along the column. It is obvious that the velocity of the inside flow path is higher than the outside one because both experience the same pressure gradient but different flow path lengths due to coiling.

For an open circular cross-sectional coiled column the additional zone broadening, in terms of plate height, due to this racetrack effect may be expressed as[8]

$$H_{coil} = \frac{7}{12}\frac{vr^4}{D_gD^2} \quad (26)$$

The dependence of $H_{coil}$ on the second power of $(r^2/D)$ enables one to minimize the racetrack effect simply by decreasing this ratio. The coil as mentioned in the previous example will contribute to the extra plate height, $H_{coil}$, by less than 0.000 56 cm at the flow rate of 386 cm/s, or a Reynolds number of about 80.

**(C) End Effect.** In general, end effects are the most important extra zone broadening factor in chromatography systems. The efficiency of a chromatography system may be evaluated by the contribution of its end effects to its total plate height. Appreciable end effects will generally skew the eluted peak and the efficiency of separation is normally poor.

End effects include the zone broadening due to finite volume of the injection port, the detector, and the joints and any dead pockets, etc. Giddings and Seager[3] provide a method for correction of this end effect. However, as mentioned earlier, the experimental exercise is difficult for a normal GC system and routine operation.

Qualitatively, the significance of the end effect of a GC system can be simply indicated by comparing the $D_g^*$ value obtained by using two different columns by the proposed method. Identical $D_g^*$ values should be obtained if the zone dispersion is due only to axial molecular diffusion and the effect of nonuniform flow profile. The advantages of this method are that, (1) it is simpler in comparison to Giddings' method, (2)

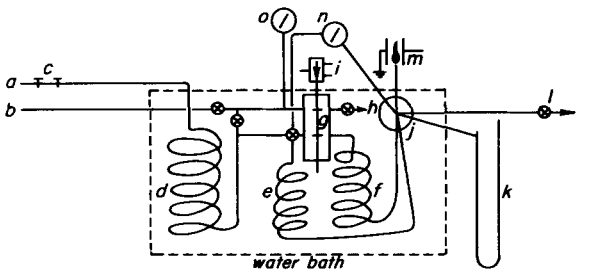


**Figure 1.** Flow diagram of gas chromatography system: (a) helium inlet; (b) sample diffusant inlet; (c) needle valves; (d) preheating column; (e) bypass column; (f) main measuring column; (g) sampling valve; (h) exit valve from sampling stream; (i) air piston; (j) stream splitter; (k) mercury barometer; (l) exit and outlet pressure valve; (m) flame ionization detector; (n) differential pressure transducer; (o) pressure gauge.

the experimental conditions do not have to be identical, and (3) the eluted peak does not have to be Gaussian.

**(D) Additional Causes of Error.** Other factors which may affect zone dispersion or the shape of the peak in all forms of GC system may be neglected when a small enough sample is employed. Among these, the concentration effect on $D_g$, the linearity of the electronics, and the buoyant effect of the solute-solvent pair, etc., needed to be carefully estimated and chosen.

## Experimental Section

A high-pressure gas-chromatography system was designed and built in this laboratory. The chromatograph has the advantage of working either under high pressure or under atmospheric pressure. It also can be operated under the condition of the arrested elution method or the continuous elution method. The flow diagram is given in Figure 1.

Helium carrier gas supply was controlled at 60 psi gauge pressure at the regulator. The flow rate of the carrier stream was precisely controlled (precision was found to be within 0.03% for six consecutive studies) by two needle valves located just in front of the preconditioning column, and by a needle valve at the exit (this needle valve is replaced by a specially designed control valve for high-pressure work up to 30 000 psi). Flow rate of the carrier stream was measured by computing the first moment of the elution peak.

The preconditioning column has a dimension of 50 ft × 0.25 in. o.d. × 0.120 in. i.d. It serves the purpose of preheating the carrier gas and also serves as a buffer system for the stability of pressure and flow rate.

The length and radius of the main column were measured by weighing the mercury contained within the void volume of the column and comparing against the weight of mercury inside a short column cut from the same delivery whose length can be precisely measured by using an engineering ruler. A 316 stainless steel column with an effective length of 461.98 cm was employed in this study. The radius of the column was calculated by using the above obtained data and the density data of mercury at that temperature. Identical values of 0.1096 cm were obtained for both columns. The curvature of both columns studied here was 10 cm.

The pressure at the outlet of the column was measured by a mercury barometer. The pressure gradient between the inlet and outlet of the column was measured by using a 1.0 psi differential pressure transducer (Model KP 15, Whittaker Corp., Hollywood, Calif.) with a precision of 0.1%.

The detail of a splitter at the end of the column is given in Figure 2. It was found that the designing of the splitter may be the key point for obtaining an ideal elution peak. A 0.002 in. i.d. × 0.006 in. o.d. stainless steel capillary tube connecting the FID jet and the column (extended 2 in. into the column) was found to be the best design in eliminating tailing of the peak due to end effect, back diffusion, and the disturbance of the flow profile at the splitter.

The flame ionization detector and the electronics were designed and built in this laboratory. The dead volume between the end of the column and the flame jet was measured to be 0.916 μl. The detection limit and time constant of this home made detector is about $10^{-10}$ g/s and $10^{-3}$ s, respectively.

The sample used here was methane gas (S.P) supplied by Matheson

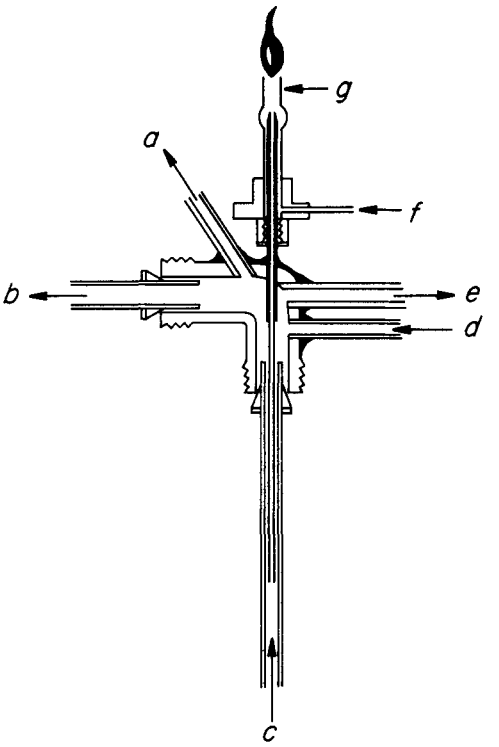


**Figure 2.** Stream splitter and flame ionization detector: (a) to differential pressure transducer; (b) to barometer; (c) from column; (d) from bypass; (e) to outlet pressure valve and regulator; (f) hydrogen inlet; (g) flame ionization detector jet.

Gas Products. Helium gas (99.995% purity) was used as carrier gas.

A special designed sampling valve was designed and built in this laboratory. The advantages of this sampling valve are that: (1) it is easy to maintain; (2) it can be operated both under high and low pressure; (3) the column was connected directly to the sampling valve, which minimized the dead volume; (4) the dead volume of the valve is about 0.904 μl; and (5) the injection speed can be controlled by adjusting the air pressure which drives the sample injection piston. The diagram of this sampling valve is shown in Figure 3.

A trace amount of sample was injected directly into the entrance of the column. The concentration profile of the eluted peak was detected by the FID system. The current source output from the detector was converted to voltage and amplified to the magnitude of about 1 V, and collected directly through a computer interface and stored in the disk memory system of the CDC computer at Oregon State University.

Temperature was precisely controlled at 25 ± 0.02 °C by a Masterline Refrigerated and Heated Bath (Model 2095, Forma Scientific, Inc., Ohio). Diluted aqueous solution of phenol was employed here as a medium for heat transfer, the phenol serving as an inhibitor for bacteria growth.

The continuous elution method was carried out in the same fashion as the conventional GC method. Flow rate was varied by adjusting the needle valves in both the inlet and outlet of the column. Column pressure was kept about constant when the flow rate was varied. The total elution time of the sample zone was measured by the timing system of the computer interface with a precision of 0.01%.

For the arrested elution method, a bypass system was used to maintain constant pressure in the column. The length of the bypass column was adjusted to have the same flow resistance as the main column so that the outlet of the column did not vary when the flow of the carrier in the main column was switched to the bypass column.

About 1000 data points were collected for each elution peak. Data are first smoothed by a nine-points quadratic-cubic smooth routine[9] to eliminate electronic noise. Area, first moment, second moment, third moment, fourth moment, skewness, kurtosis, velocity, and the dispersion coefficient are then computed by using numerical methods (Simpson's Rule). For the purpose of a least-squares fit of the data points into the theoretical equation, the data points were assembled into about 200 by using a sequential 7 to 11 data points averaging

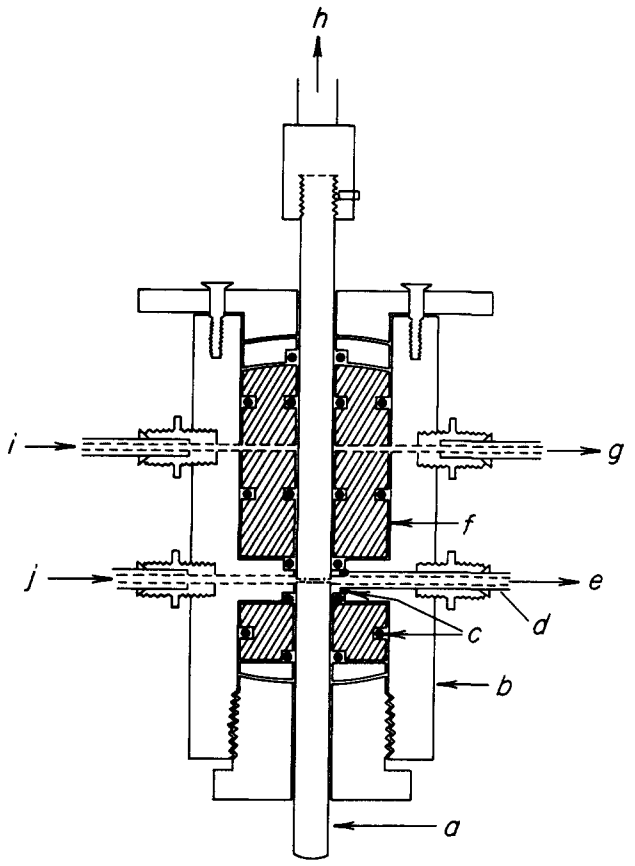


**Figure 3.** Main body of sampling system: (a) stainless steel shaft; (b) stainless steel housing; (c) O-rings; (d) column; (e) to column; (f) graphite-filled Teflon; (g) sample stream exit; (h) to piston; (i) sample stream inlet; (j) carrier gas inlet.

routine. A least-squares fit program was then employed to compute the least-squares fit $D_g$* value.

## Results and Discussion

Highly precise and accurate $D_g$* values can only be obtained from a GC system which has a minimum contribution to the zone broadening due to its end effect, secondary flow effect, racetrack effect, concentration effect, and the others. Direct calculation showed that the column employed in this study made no extra zone broadening due to secondary flow effect at the condition we employed, and about 0.0003% due to racetrack effect. The total dead volume as mentioned before is less than 2 $\mu$l, which contributes less than 0.015% the total effective column volume. It is obvious that this small dead volume cannot contribute to a significant zone-broadening effect, except the flow profile was disturbed and back diffusion occurred at the inlet and outlet of the system. The effect of those extra zone-broadening factors can easily be observed from the skewness of the eluted peak, the significant difference between the sum of the square of the experimental and the theoretical $C$ values, and the standard error of the fitted parameter, $D_g$*. It was observed that the extension of a 0.002 in. capillary tube about 2 in. into the end of the column improved the difference between the sum of the squares of the experimental and the theoretical concentration values from $10^2$-$10^4$ to $10^{-2}$-$10^1$ in the total sum squares of concentration values of the order of $10^7$ to $10^9$. Also, the standard error of $D_g$* from least-squares fit to single peak was improved from $10^{-1}$-$10^{-2}$ to $10^{-3}$-$10^{-5}$.

$D_g$* values obtained from both long (461.98 cm) and short (358.52 cm) columns are tabulated in Tables I and II. It is shown that when the 461.98-cm column was employed, 14 continuous elution measurements gave an average $D_g$* value of 0.6776 cm$^2$/s and a standard deviation of 0.0014 absolute or 0.22% relative. The arrested elution measurements using the same column gave an average of 0.6735 cm$^2$/s and a standard deviation of 0.000 79 absolute or 0.12% relative. It is interesting that all the $D_g$* values obtained by the arrested elution method were smaller than those obtained by continuous elution methods, and the standard error of each measurement was also smaller in the arrested elution method. This may be due to the reason that in the continuous elution method the column length was too short to ensure that the effect of flow fluctuation can be neglected or that the Taylor equation did not accurately represent the dispersion in our imperfect tube.

**Table I.** Binary Molecular Diffusion Coefficients ($CH_4$-He) Obtained from the Continuous Elution Method with a 461.98-cm Column and at 25 ± 0.02 °C

| Velocity, cm/s | $D_g$*, cm$^2$/s, from least-squares fit | Standard error of $D_g$* from least-squares fit |
|---|---|---|
| 2.1597 | 0.6772 | $5.0 \times 10^{-4}$ |
| 2.1623 | 0.6782 | $5.2 \times 10^{-4}$ |
| 2.5805 | 0.6780 | $5.4 \times 10^{-4}$ |
| 2.5811 | 0.6751 | $4.2 \times 10^{-4}$ |
| 3.0768 | 0.6782 | $5.8 \times 10^{-4}$ |
| 3.1498 | 0.6785 | $5.7 \times 10^{-4}$ |
| 3.1512 | 0.6790 | $5.8 \times 10^{-4}$ |
| 3.4204 | 0.6778 | $3.5 \times 10^{-4}$ |
| 3.5178 | 0.6756 | $3.2 \times 10^{-4}$ |
| 3.5216 | 0.6772 | $4.3 \times 10^{-4}$ |
| 3.9715 | 0.6769 | $7.0 \times 10^{-4}$ |
| 3.9758 | 0.6792 | $8.5 \times 10^{-4}$ |
| 4.4455 | 0.6799 | $4.7 \times 10^{-4}$ |
| 4.4472 | 0.6758 | $4.2 \times 10^{-4}$ |
| | Av 0.6776 | |
| | SD 0.001 410 | |

**Table II.** Binary Molecular Diffusion Coefficient ($CH_4$-He) Obtained from the Arrested Elution Method with a 461.98-cm Column at 25 ± 0.02 °C

| Velocity, cm/s | Arrested time, s | $D_g$*, cm$^2$/s, from least squares fit | Standard error of $D_g$* from least-squares fit |
|---|---|---|---|
| 1.6663 | 300 | 0.6739 | $6.01 \times 10^{-4}$ |
| 1.6658 | 350 | 0.6747 | $7.77 \times 10^{-4}$ |
| 1.6669 | 500 | 0.6733 | $8.33 \times 10^{-4}$ |
| 1.6660 | 550 | 0.6730 | $6.59 \times 10^{-4}$ |
| 1.6622 | 700 | 0.6731 | $8.63 \times 10^{-4}$ |
| 1.6678 | 850 | 0.6740 | $6.76 \times 10^{-4}$ |
| 1.6641 | 900 | 0.6723 | $5.80 \times 10^{-4}$ |
| | | Av 0.6735 | |
| | | SD 0.000 788 | |

Our figure of 0.674 ± 0.002 for $CH_4$ in He at 25 °C is 2% lower than that derived from Marrero and Mason's empirical equation[5] derived from fitting published data. This is well within their estimated uncertainty of 3%. It agrees well with the value of 0.675 obtained with the data published by Carswell and Stryland[10] and Hu and Kobayashi's value[11] of 0.679 ± 0.006.

The speed of this method is very much faster than all the conventional methods in determining molecular diffusivity. The shorter column length and on-line data collection and reduction enhance the speed of the method to about 7 min/determination and calculation of $D_g$* value.

**Acknowledgment.** This work was supported by NSF Grant GP15430.

## References and Notes

(1) J. C. Giddings and S. L. Seager, *J. Chem. Phys.*, **33**, 1579 (1960).
(2) J. C. Giddings and S. L. Seager, *J. Chem. Phys.*, **35**, 2242 (1961).
(3) J. C. Giddings and S. L. Seager, *Ind. Eng. Chem., Fundam.*, **1**, 277 (1962).
(4) J. H. Knox and L. McLaren, *Anal. Chem.*, **36**, 1477 (1964).
(5) T. R. Marrero and E. A. Mason, *J. Phys. Chem. Ref. Data*, **1**, 3 (1972).
(6) V. R. Maynard and E. Grushka, *Adv. Chromatogr.*, **12**, (1975).
(7) C. M. White, *Proc. R. Soc. London, Ser. A*, **123**, 645 (1929).
(8) J. C. Giddings, *J. Chromatogr.*, **1**, 520 (1960).
(9) A. Savitzky and M. J. E. Golay, *Anal. Chem.*, **36**, 1627 (1964).
(10) A. J. Carswell and J. C. Stryland, *Can. J. Phys.*, **41**, 708 (1963).
(11) A. T. Hu and R. Kobayashi, *J. Chem. Eng. Data*, **115**, 328 (1970).


# Representations of Molecular Force Fields. 2. A Modified Urey–Bradley Field and an Examination of Allinger's Gauche Hydrogen Hypothesis


**Susan Fitzwater and L. S. Bartell***

*Contribution from the Department of Chemistry, The University of Michigan, Ann Arbor, Michigan 48109.*

*Received December 22, 1975*


**Abstract:** A modified Urey-Bradley force field for hydrocarbons, designated MUB-2, has been constructed for application in the field of "molecular mechanics". The initial aim of this research was to incorporate as realistic nonbonded potential energy functions as are presently possible in a pairwise additive formulation in order to investigate the plausibility of Allinger's new gauche-hydrogen interaction basis of conformational analysis. The resultant force field, derived from Kochanski's $H_2 \cdots H_2$ quantum calculations and various experimental observations, yielded an energy for H···H interactions similar to that of Allinger's field at the crucial 2.6 Å internuclear distance for vicinal hydrogens. Nevertheless, considered in its entirety, it supported the conventional interpretation rather than Allinger's, for reasons that are discussed. Field MUB-2 was designed to be nominally of the "consistent force field" type though it is too sparing in parameters to reproduce vibrational and thermochemical quantities with high accuracy. It gives an excellent account of structures and structural trends in the cases it has been applied to, being superior in these cases to alternative published fields. It gives a fair account of isomerization energies, being inferior to several more optimized fields containing a greater number of adjustable parameters than does MUB-2. It gives correct magnitudes of vibrational frequencies but poor splittings due to its neglect of certain interaction constants. One area in which MUB-2 outperforms alternative fields for molecular mechanics is exemplified in its successful semiquantitative prediction of certain unknown force constants for ethane that were later calculated by ab initio molecular orbital methods. These constants include a variety of bend and stretch-bend couplings, harmonic and anharmonic, which are not represented in the other fields, and which stem in MUB-2 from geminal H···H and C···H nonbonded interactions. The new field is far from a fully optimized field but it furnishes useful clues and guidelines for future advances in molecular mechanics.


## I. Introduction

In studies of conformational analysis there has been widespread use of the "molecular mechanics" potential energy minimization method.[1] Many different model force fields have been proposed in attempts to get a satisfactory analytical representation but in no sense has a final, accepted force field emerged. This is because so little is known about force fields that not even for a molecule as simple as *ethane* are the true potential constants known from experiments![2] Therefore, by necessity, all proposed fields are greatly simplified representations containing only a fraction of the parameters allowable in a general representation. Adding to the difficulty is the fact that, when attempts are made to refine parameters in these simplified fields by comparisons of calculated quantities with experiment, high parameter correlations, in addition to the aforementioned systematic errors of truncation, prevent the derivation of a reliable and uniquely appropriate set of potential constants. Different workers with different points of view adopt strikingly different force fields. In many comparisons the results of the different force fields are in fair agreement.

Naturally, the above situation has led to diverse interpretations of trends in molecular properties. One of the more intriguing recent interpretations is Allinger's challenge to the popular idea that gauche conformations are destabilized relative to anti because of 1···6 hydrogen repulsions between gauche methyl or methylene groups.[3] Allinger maintains that the gauche destabilizations instead stem in large measure from 1···4 (vicinal) interactions between hydrogens bonded to the carbons forming the axis of internal rotation.

Since gauche destabilization is one of the cornerstones of conformational analysis and since new theoretical information[2,4] has become available since Allinger's 1973 field was constructed, it seemed timely to test Allinger's assertion that his conclusions are not dependent on the exact parameterization of the force field. It was clear from the outset that his conclusions were not consistent with the reasonably successful force field MUB-1[5] (sometimes referred to as JTB). It was of great interest to find whether his conclusions were compatible with a new force field constructed on a firmer basis than the MUB-1 force field, with new theoretical constraints built in to uncouple the otherwise highly correlated nonbonded interaction functions that are so crucial in tests of Allinger's hypothesis.

The new force field, which we designate as MUB-2, is not intended to be a final or even a fully optimized field within its own limited framework. It is certainly inferior to, for example, the CFF (consistent force field) of Ermer and Lifson[6] in representing vibrational frequencies. It is likely to have as rational a basis as presently exists, however, for assessing the role of H···H interactions in molecular mechanics. For this reason it is worthwhile to describe the construction of the model. The key points are outlined in section II and details are given in